Available online at www.sciencedirect.com

Chemical Engineering Research and Design

journal homepage: www.elsevier.com/locate/cherd

Modelling the required membrane selectivity for NO_3^- recovery from effluent also containing Cl^-, while saving water

D. Chinello[a,b,*], A. Myrstad[c], L.C.P.M. de Smet[a,b], H. Miedema[a]

[a] Wetsus, European Centre of Excellence for Sustainable Water Technology, Oostergoweg 9, Leeuwarden 8911 MA, the Netherlands

[b] Laboratory of Organic Chemistry, Wageningen University, Stippeneng 4, Wageningen 6708 WE, the Netherlands

[c] Yara Porsgrunn (Yara Norge AS), Hydrovegen 55, N-3936 Porsgrunn, Norway

ARTICLE INFO

Article history:
Received 10 January 2023
Received in revised form 6 March 2023
Accepted 19 March 2023
Available online 29 March 2023

Keywords:
NO_3^- recovery
NO_3^- over Cl^- membrane selectivity
Water purification
Mass balance
Modelling
Fertilizer production

ABSTRACT

We present a general outline for the selective recovery of NO_3^- from a (waste) water stream also containing Cl^-. The key element of the technology introduced and simulated here is a membrane unit demonstrating NO_3^- over Cl^- permeation selectivity. The membrane is hypothesized to be hydrophobic and with that exploiting the difference in dehydration energy between NO_3^- and Cl^-. Apart from NO_3^- recovery, the process also aims to reduce water consumption. Based on a generic outline of the process, the key parameters are defined, being the NO_3^-/Cl^- concentration ratio in the (waste) stream, the fraction of NO_3^- and water recovered, and the selectivity of the membrane. The sensitivity of the separation process to these four parameters is evaluated. In the second part of the paper, the same principles are applied to a real-life process, i.e., NO_3^- recovery from the effluent (waste) water of a fertilizer production plant. The aim was to calculate the membrane NO_3^-/Cl^- permeation selectivity required to recover 90% of NO_3^-, given a threshold value for the Cl^- concentration in the permeate stream and recycle 30% of the water, starting from two different NO_3^-/Cl^- concentration ratios in the effluent (waste) water. With 51 mM Cl^- in the effluent (waste) water and a Cl^- threshold of 9.9 mM, a membrane selectivity of 3 suffices. The required selectivity increases to 30 when the Cl^- in the effluent (waste) water is 200 mM and the Cl^- threshold is 4.2 mM. Reported NO_3^-/Cl^- membrane selectivities are still modest, with a maximal selectivity found in literature of 3. Strategies to develop membranes of significant higher selectivity are briefly discussed.

1. Introduction

Nitrogen is an essential nutrient for agriculture. In 2020 its consumption was estimated to be 10 million tonnes in the EU alone, 6.9% above its consumption in 2010 ("Agri-environmental indicator - mineral fertiliser consumption.", 2022). The conversion of N_2 to ammonia, an essential compound for fertilizer production, via the Haber-Bosch process is not only

* Corresponding author at: Wetsus, European Centre of Excellence for Sustainable Water Technology, Oostergoweg 9, Leeuwarden 8911 MA, the Netherlands.
E-mail address: daniele.chinello@wetsus.nl (D. Chinello).

https://doi.org/10.1016/j.cherd.2023.03.038

energy intensive but also responsible for no less than 1.5% of the total worldwide CO_2 emission (Kyriakou et al., 2020). With an increasing global population – by 2060, the world population will reach 10 billion ("World Population Prospects, 2019 Highlights.pdf." 2022) – and the decrease in agricultural production due to climate change (Wang et al., 2020), pests (Skendžić et al., 2021), and lack of nutrients, the need of using fertilizers to sustain crop production will only increase further. However, not all applied fertilizer is actually taken up by crops. As an example case, in 2015 the nitrogen use efficiency (NUE) of cereal was estimated to be just 35% (Omara et al., 2019). Due to precipitation, excess fertilizer leaches out of the soil, causing eutrophication of surface waters with all its detrimental effects (Dodds and Smith, 2016). Furthermore, the presence of nitrogen oxides, such as nitrate (NO_3^-), in drinking water is responsible for infant methemoglobinemia (also known as blue baby syndrome) and increases the risk of cancer (Essien et al., 2022) and birth defects (Ward et al., 2018).

Currently used wastewater treatment technologies remove nitrogen by conversion of N-species to gaseous N_2 (Ni et al., 2017). However, these nitrification/denitrification processes deal with high costs, high chemical use, and by-product formation such as N_2O (Ye et al., 2018) and Cl_2. Moreover, the conversion to N_2 is irreversible, resulting in removing biologically directly available nitrogen from the ecosystem. From the point of view of both economics and sustainability, an attractive alternative is the selective recovery of nitrogen. To do so, we here explore the potential and requirements of membrane technology to selectively recover NO_3^-.

Together with phosphorus (P) and potassium (K), nitrogen (N) is the main component of NPK fertilizers; chloride is present as well because potassium chloride (KCl) is the source of potassium. The co-presence of Cl^- makes the recovery of NO_3^- challenging because both ion species have the same valence. However, there is a difference in the (effective) crystal radius and by implication in the dehydration energy. With an ionic radius of 0.181 nm for Cl^- and 0.264 nm for NO_3^- (Nightingale, 1959), the latter has a lower dehydration energy (Smith, 1977).

In membrane technology, differences in dehydration energy can be exploited to separate ion species. As shown in previous studies (Mubita et al., 2020; Qian et al., 2020, 2022; Vaselbehagh et al., 2016; Sodaye et al., 2007; Kikhavani et al., 2014; Sata, 2000), the transport of ions with low dehydration energy is enhanced by increasing the membrane hydrophobicity. Therefore, in this study, we hypothesize and introduce a membrane unit possessing a hydrophobic membrane with a permeation preference of NO_3^- over Cl^- because of the lower dehydration energy of the former ion species. Furthermore, it is envisaged that the membrane operates in an electrodialysis setting.

This paper consists of two parts. The first one describes and discusses a rather basic outline of a process for the separation of NO_3^- from Cl^- using membrane technology. The most relevant process parameters are evaluated. In the second part of the paper, we switch to a real-life application, using some of the findings discussed in the first part. Here, we investigate the recovery of NO_3^- from the effluent (waste) water of a fertilizer plant while saving 30% of fresh water.

2. Materials and methods

2.1. System description

Fig. 1 shows a general outline of a membrane-based process for the selective separation of NO_3^- from Cl^-. The (waste) water stream containing the two ion species, from here on labelled the feed stream, enters the system in the mixer, where fresh and recycled water are added to the extent to keep the volumetric flow constant. The resulting stream (reference point #0) is sent to the membrane unit responsible for the NO_3^- recovery and producing a permeate stream (reference point #1) relatively rich in NO_3^-. Depending on the membrane selectivity, this stream is more or less contaminated with Cl^-. The retentate stream (reference point #2), relatively rich in Cl^-, is split (reference point #3) and, in order to minimize the fresh water consumption, partly recycled and directed towards the mixer.

In the system, four reference points are distinguished:

- point #0: where fresh water, the feed stream, and recycled water are mixed;
- point #1: water stream after filtration by the membrane unit (permeate side);
- point #2: water stream after filtration by the membrane unit (retentate side);
- point #3: water stream after splitting, re-entering the mixer.

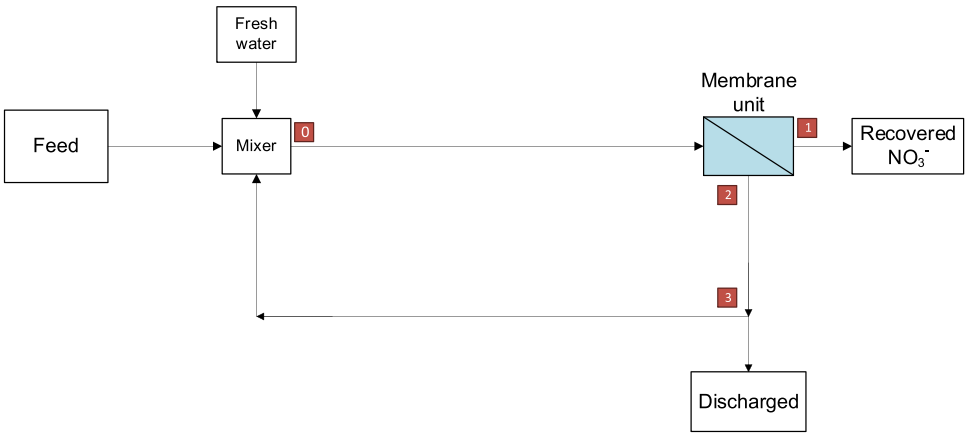

Fig. 1 – General outline of a membrane-based process for the selective recovery of NO_3^- from a water stream also containing Cl^-. Reference points #0–3 are indicated and further explained in the text.

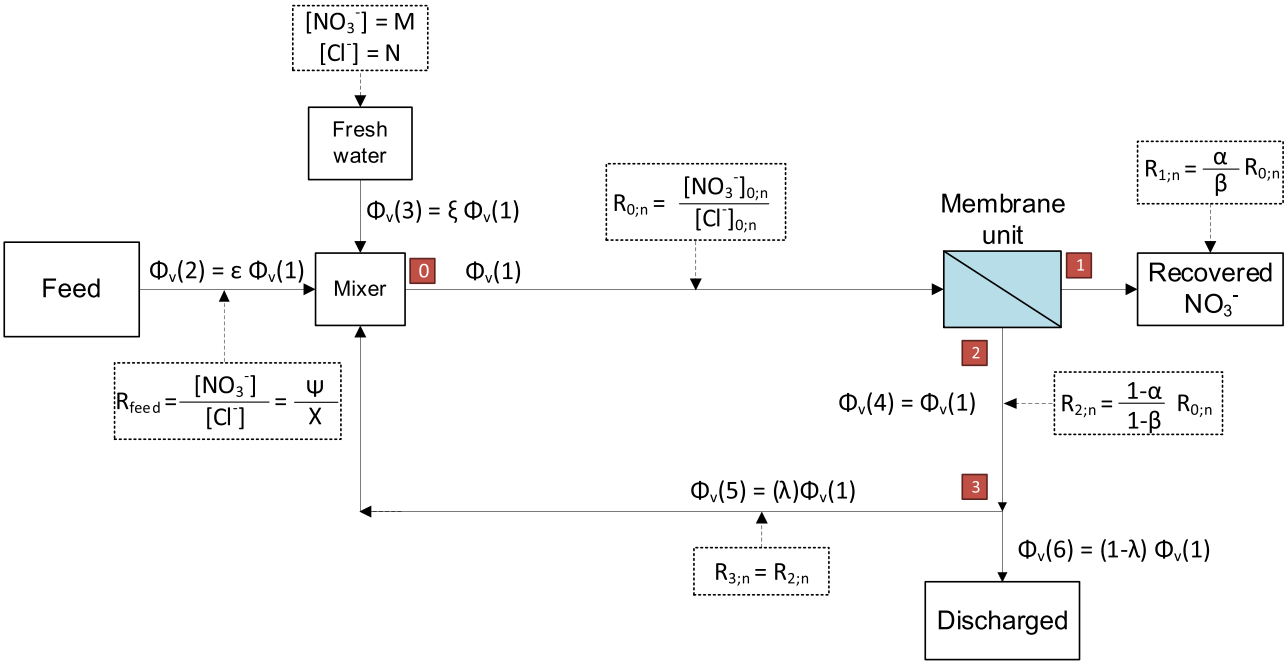

Fig. 2 – Outline of Fig. 1, complemented with volumetric flows Φv(1)-Φv(6) and all relevant process parameters.

The model calculates the NO_3^-/Cl^- concentration ratio (indicated with the letter R) at the four reference points at a range of set membrane selectivity values. This way, we can define the NO_3^- over Cl^- permeation membrane selectivity required to achieve the desired concentration ratio value at reference point #1.

The nomenclature adopted throughout this study is based on the use of two indices, the first representing the reference point and the second the cycle number. For instance, $R_{2;4}$ refers to the NO_3^-/Cl^- concentration ratio at reference point #2 during the fourth cycle:

$$R_{2;4} = \frac{[NO_3^-]_{2;4}}{[Cl^-]_{2;4}}$$

2.2. Mass balance

Fig. 2 shows the basic outline of Fig. 1, complemented with all relevant parameters referred to in this study, which are reported in Table 1. The volumetric flow leaving point #0 and entering the membrane unit remains constant through the cycles.

For the first cycle, it has been assumed that the composition at point #0 is 50% feed stream and 50% fresh water. As remarked, after the first cycle, and in order to limit the fresh water consumption, some of the retentate stream ($\Phi_v(5)$, reference point #3) is recycled. This fraction (λ) will be varied in the simulations from 0.5 to 0 to study the influence of the Cl^- build-up in the system on the required membrane selectivity. Moreover, for all cycles, the fraction of the feed stream entering the mixer has been fixed at 0.5.

2.2.1. First cycle (n = 1)

2.2.1.1. Reference point #0. As mentioned previously, the composition at point #0 is 50% feed stream (ε_1 = 0.5) and 50% fresh water (ξ_1 = 0.5), resulting in the following volumetric flow:

$$\Phi_v(1) = \Phi_v(2) + \Phi_v(3) = \varepsilon_1 \Phi_v(1) + \xi_1 \Phi_v(1) \quad (1)$$

With Ψ and X representing the concentration of NO_3^- and Cl^- in the feed stream, and M and N the concentration of NO_3^- and Cl^- in fresh water, the NO_3^- and Cl^- mass balances read as follows:

Table 1 – List of the parameters used for this study.

Variable	Description	Variable	Description
Φ_v	Volumetric flow	ε_1	Fraction of feed stream entering at point #0 for the 1st cycle
Ψ	NO_3^- concentration in the feed	ε_n	Fraction of feed stream entering at point #0 for cycle number n (n > 1)
X	Cl^- concentration in the feed	ξ_1	Fraction of fresh water entering at point #0 for the 1st cycle
R_{feed}	NO_3^-/Cl^- concentration ratio in the feed: $R_{feed} = \Psi/X$	ξ_n	Fraction of fresh water entering at point #0 for cycles number n (n > 1)
$R_{m,n}$	NO_3^-/Cl^- concentration at reference point #m in cycle #n	α	Fraction of NO_3^- removed by the membrane system
M	NO_3^- concentration in fresh water	β	Fraction of Cl^- removed by the membrane system
N	Cl^- concentration in fresh water	γ	NO_3^- over Cl^- permeation selectivity of the membrane system: α/β
		λ	Fraction of water recycled

$$\Phi_v(1)[NO_3^-]_{0;1} = \varepsilon_1\Phi_v(1)\Psi + \xi_1\Phi_v(1)M \quad (2)$$

$$[NO_3^-]_{0;1} = \varepsilon_1\Psi + \xi_1 M \quad (3)$$

$$\Phi_v(1)[Cl^-]_{0;1} = \varepsilon_1\Phi_v(1)X + \xi_1\Phi_v(1)N \quad (4)$$

$$[Cl^-]_{0;1} = \varepsilon_1 X + \xi_1 N \quad (5)$$

Therefore, the NO_3^-/Cl^- concentration ratio is defined by:

$$R_{0;1} = \frac{[NO_3^-]_{0;1}}{[Cl^-]_{0;1}} = \frac{\varepsilon_1\Psi + \xi_1 M}{\varepsilon_1 X + \xi_1 N} \quad (6)$$

2.2.1.2. *Reference point #1.* Reference point #1 is positioned at the permeate side of the membrane unit. With α and β representing the fractions of feed NO_3^- and Cl^- that permeate the membrane, the concentration ratio of these two ion species is:

$$R_{1;1} = \frac{[NO_3^-]_{1;1}}{[Cl^-]_{1;1}} = \frac{\alpha}{\beta}R_{0;1} = \gamma R_{0;1} \quad (7)$$

where γ represents the membrane permeation selectivity:

$$\gamma = \frac{\alpha}{\beta} \quad (8)$$

It can easily be appreciated that γ is indeed a measure of the selectivity of the membrane. Indeed, the ratio of the number of moles of NO_3^- and Cl^- passing the membrane per unit of time, $n_{NO_3^-}$ and n_{Cl^-}, is given by:

$$\frac{n_{NO_3^-}}{n_{Cl^-}} = \frac{\alpha[NO_3^-]_{0;n}}{\beta[Cl^-]_{0;n}} \quad (9)$$

To normalize this ratio for the effect of concentration, this number needs to be multiplied by the inverse ratio of their feed concentrations, resulting in:

$$\frac{n_{NO_3^-}}{n_{Cl^-}}\frac{[Cl^-]_{0;n}}{[NO_3^-]_{0;n}} = \frac{\alpha[NO_3^-]_{0;n}}{\beta[Cl^-]_{0;n}}\frac{[Cl^-]_{0;n}}{[NO_3^-]_{0;n}} = \frac{\alpha}{\beta} = \gamma \quad (10)$$

2.2.1.3. *Reference point #2.* Reference point #2 is located downstream the membrane unit, as is reference point #1, but at the retentate side instead. Here the concentration ratio is given by:

$$R_{2;1} = \frac{[NO_3^-]_{2;1}}{[Cl^-]_{2;1}} = \frac{(1-\alpha)}{(1-\beta)}R_{0;1} \quad (11)$$

Because of the hydrophobic nature of the proposed membrane, any potential water transport over the membrane is neglected, resulting in a volumetric flow balance of:

$$\Phi_v(4) = \Phi_v(1) \quad (12)$$

2.2.1.4. *Reference point #3.* At this point, stream $\Phi_v(4)$ is split into two streams. One is discharged and one is recycled and led to the mixer. Given that a fraction (λ) is recycled, the volumetric flow balance reads:

$$\Phi_v(5) = \lambda\Phi_v(1) \quad (13)$$

Compared to reference point #2, the NO_3^-/Cl^- concentration ratio at point #3 is the same:

$$R_{3;1} = R_{2;1} = \frac{[NO_3^-]_{3;1}}{[Cl^-]_{3;1}} \quad (14)$$

2.2.2. *Second cycle ($n = 2$)*

2.2.2.1. *Reference point #0.* The calculations for the 2nd cycle, and for that matter for all cycles that follow as well, are essentially the same as those for the first cycle. The main difference with the first cycle regards the volumetric flow balance at the reference point #0, considering that a fraction (λ) of the retentate stream ($\Phi_v(5)$) has been recycled, resulting in:

$$\Phi_v(1) = \Phi_v(2) + \Phi_v(3) + \Phi_v(5) \quad (15)$$

or, expressed slightly differently, in:

$$\Phi_v(1) = \varepsilon_2\Phi_v(1) + \xi_2\Phi_v(1) + \lambda\Phi_v(1) \quad (16)$$

The NO_3^- and Cl^- mass balances are:

$$[NO_3^-]_{0;2} = \varepsilon_2\Psi + \xi_2 M + \lambda[NO_3^-]_{3;1} \quad (17)$$

$$[Cl^-]_{0;2} = \varepsilon_2 X + \xi_2 N + \lambda[Cl^-]_{3;1} \quad (18)$$

where:

$$\varepsilon_2 = \varepsilon_1 = 0.5 \quad (19)$$

and

$$\xi_2 = 1 - \varepsilon_2 - \lambda \quad (20)$$

Based on Eq. (17 and 18), $R_{0;2}$ is given by:

$$\frac{[NO_3^-]_{0;2}}{[Cl^-]_{0;2}} = R_{0;2} = \frac{\varepsilon_2\Psi + \xi_2 M + \lambda[NO_3^-]_{3;1}}{\varepsilon_2 X + \xi_2 N + \lambda[Cl^-]_{3;1}} \quad (21)$$

The expressions regarding reference points #1 to #3 are similar to those for the first cycle, as outlined in the next sections.

2.2.2.2. *Reference point #1*

$$\frac{[NO_3^-]_{1;2}}{[Cl^-]_{1;2}} = R_{1;2} = \frac{\alpha}{\beta}R_{0;2} = \gamma R_{0;2} \quad (22)$$

2.2.2.3. *Reference point #2*

$$\frac{[NO_3^-]_{2;2}}{[Cl^-]_{2;2}} = R_{2;2} = \frac{(1-\alpha)}{(1-\beta)}R_{0;2} \quad (23)$$

$$\Phi_v(4) = \Phi_v(1) \quad (24)$$

2.2.2.4. *Reference point #3*

$$\Phi_v(5) = \lambda\Phi_v(1) \quad (25)$$

$$\frac{[NO_3^-]_{3;2}}{[Cl^-]_{3;2}} = R_{3;2} = R_{2;2} \quad (26)$$

3. Results

As evident from Section 2, the calculations require input values of a number of parameters. The following four are considered the most important ones:

- The NO_3^-/Cl^- concentration ratio in the feed (R_{feed});
- The fraction of NO_3^- (α) removed at the membrane unit;
- The membrane permeation selectivity (γ) with $\gamma = \alpha/\beta$;
- The fraction of retentate stream that is recycled (λ).

Here we will evaluate the sensitivity of the calculations to the value of each of these key parameters on the (equilibrium) value of $R_{1,n}$, that is the NO_3^-/Cl^- concentration ratio in the permeate stream of the membrane unit. The reason to

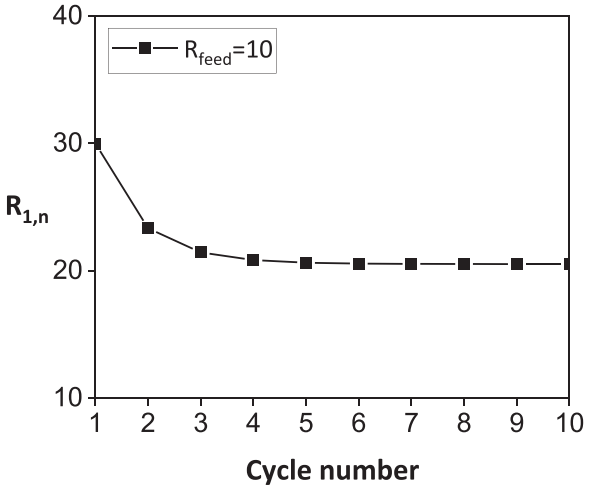

Fig. 3 – NO_3^-/Cl^- concentration ratio in the permeate stream ($R_{1,n}$) in relation to the cycle number for a NO_3^-/Cl^- concentration ratio in the feed of R_{feed} = 10. The numerical values of the other parameters used for the calculations are: α = 0.9, γ = 3, λ = 0.5.

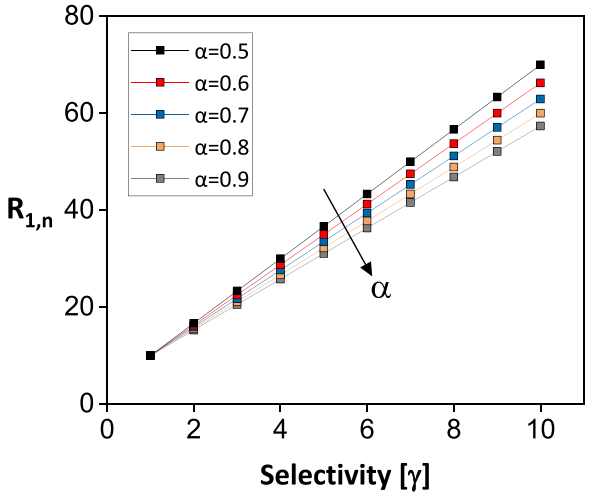

Fig. 5 – NO_3^-/Cl^- concentration ratio in the permeate stream ($R_{1,n}$) in relation to the membrane selectivity (γ) and the fraction of NO_3^- removed at the membrane unit (α) for R_{feed} = 10. The value of λ was set at 0.5. The arrow indicates the direction of increasing α.

focus on this parameter, $R_{1;n}$, is that it is a measure of the purity of the recovered NO_3^-. All graphs plot $R_{1;n}$ as a function of γ. The reason to present the data this way is that our prime aim concerns defining the required membrane selectivity in relation to the purity of the recovered NO_3^-.

As stated, the values of $R_{1,n}$ relate to steady-state conditions at which the NO_3^- and Cl^- concentrations at reference point #1 adopt their equilibrium values. The number of cycles needed to reach equilibrium is independent of the NO_3^-/Cl^- concentration ratio in the feed (R_{feed}) due to the assumption that the fraction of recovered NO_3^- is constant, and, in this case, arbitrarily set to 0.9. A model including a limited NO_3^- membrane transport capacity affects the results. Fig. 3 shows $R_{1;n}$ as function of the cycle number for R_{feed} = 10 (similar data for R_{feed} = 0.1 and 1 is shown in Fig. S1 of the Supporting Information). As shown in Fig. 3, steady-state is reached already from the fourth or fifth cycle on. Note that the decline of $R_{1;n}$ after the first cycle results from Cl^- building up in the system due to the partial recycling of the retentate stream at reference point #3 ($\Phi_v(5)$). From here on, all presented data except those of Fig. 6 refer to the equilibrium condition.

3.1. *Influence of the NO_3^-/Cl^- concentration ratio in the feed (R_{feed})*

It is expected that the higher the NO_3^-/Cl^- ratio in the feed (R_{feed}), the lower the membrane selectivity required to achieve a certain purity of the permeate stream at point #1. Calculations confirm this hypothesis. Fig. 4 shows $R_{1;n}$ as a function of the membrane selectivity (γ) at three different R_{feed} values, 0.1 and 1 (panel A) and 10 (panel B). The value of R_{feed} clearly sets a limit to the maximal value of $R_{1;n}$, that can be obtained, even at high separation ratios. For instance, the combination of R_{feed} = 1 and γ = 10 just results in a modest $R_{1;n}$ of approximately 6. Considering a tenfold excess of NO_3^- in combination with the same membrane selectivity, results in a tenfold increase of $R_{1;n}$.

3.2. *Influence of the fraction of NO_3^- removed by the membrane unit (α)*

In addition to the α/β ratio, the absolute value of α also affects $R_{1;n}$. Fig. 5 demonstrates this effect for α values ranging from 0.5 to 0.9, at γ values varying from 1 to 10, and for R_{feed} = 10

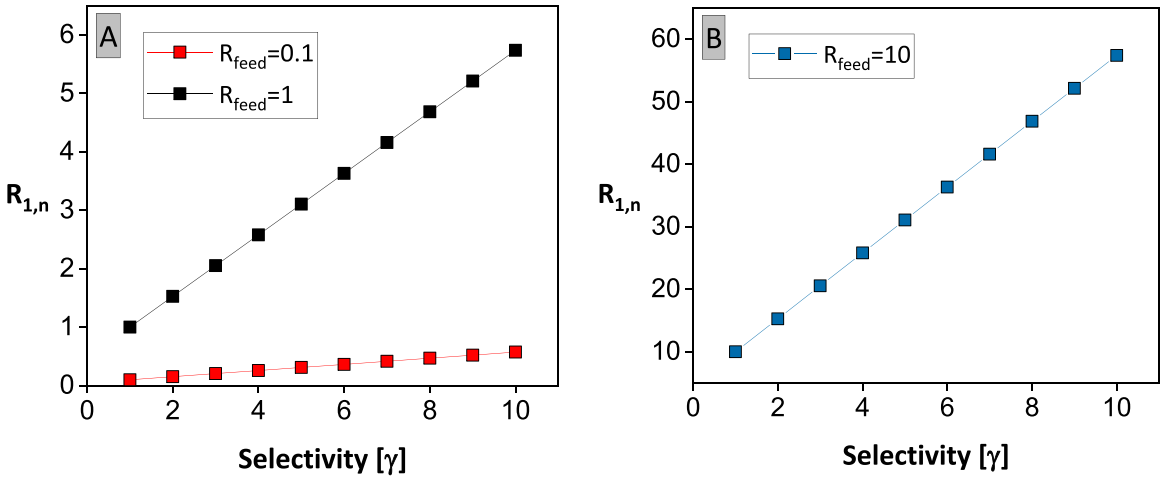

Fig. 4 – NO_3^-/Cl^- concentration ratio in the permeate stream ($R_{1,n}$) in relation to the membrane selectivity (γ) at NO_3^-/Cl^- concentration ratios in the feed (R_{feed}) of 0.1 and 1 (panel A) and 10 (panel B). In all cases the value of λ was set at 0.5.

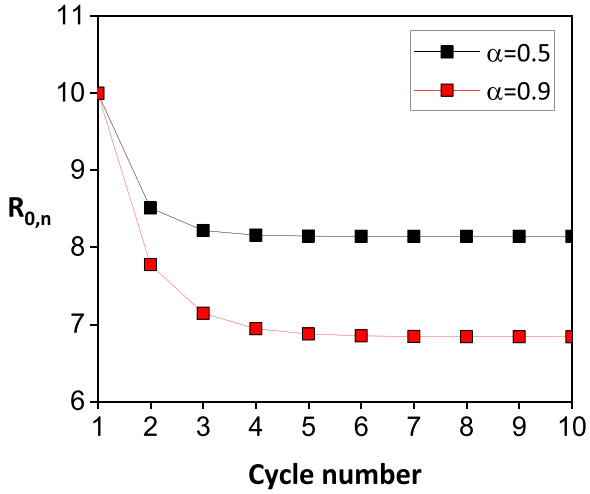

Fig. 6 – NO_3^-/Cl^- concentration at reference point #0 ($R_{0,n}$) in relation to the cycle number and the fraction of NO_3^- removed at the membrane unit (α) for R_{feed} = 10. The α values used are 0.9 and 0.5, and λ was set at 0.5.

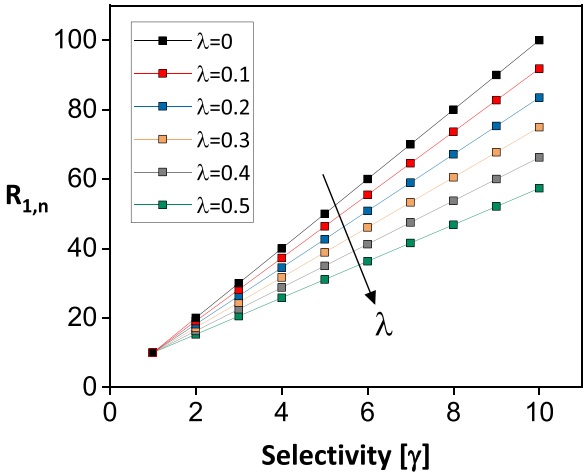

Fig. 7 – NO_3^-/Cl^- concentration ratio in the permeate stream ($R_{1,n}$) in relation to the membrane selectivity (γ) and the fraction of the retentate stream recycled (λ); for R_{feed} = 10; the value of α was set at 0.9. The arrow indicates the direction of increasing λ.

(similar data for R_{feed} = 0.1 and 1 are shown in Fig. S2 of the Supporting Information). At any given value of γ, the higher α, the lower $R_{1;n}$. The explanation for this somehow counter-intuitive result is that a higher α implies a lower $R_{0;n}$ at the start of the next cycle because stream $\Phi_v(5)$ contains less NO_3^-. Fig. 6 shows this effect. As can be concluded from **Figure 4**, $R_{1;n}$ scales linearly with R_{feed}, at any given membrane selectivity. Higher α values thus result in lower values of $R_{1;n}$, as shown in Fig. 5 for R_{feed} = 10 (similar data for R_{feed} = 0.1 and 1 is shown in Fig. S2 of the Supporting Information).

3.3. *Influence of the fraction of water recycled (λ)*

Finally, we explore the effect of the fraction of water recycled, λ. From the point of view of reducing fresh water consumption, a high λ is desirable. However, λ clearly influences the concentration of Cl^- and NO_3^- in the system as well, with a higher impact on the Cl^- concentration due to the NO_3^- recovery at the membrane unit. By implication, the membrane selectivity required to achieve a certain NO_3^-/Cl^- concentration ratio in the permeate stream ($R_{1,n}$) is influenced by λ. Fig. 7 shows $R_{1;n}$ as function of γ, for λ ranging from 0 to 0.5, and for R_{feed} value of 10, (similar data for R_{feed} = 0.1 and 1 are shown in Fig. S3 of the Supporting Information). Suppose we aim for $R_{1;n}$ = 50, according to Fig. 7 and without recycling (λ = 0), the required membrane selectivity is around 5. This number doubles when half of the stream at point #3 is recycled, i.e. with λ = 0.5.

3.4. *Application: NO_3^- recovery from a fertilizer production plant effluent*

The real-life process parameters referred to in this section relate to NPK fertilizer production of Yara in Porsgrunn (Norway). Fig. 8 schematically outlines the process of their production plant. Part of the process that is actually involved in the treatment of the effluent water generated by the fertilizer plant is indicated by the dashed red box (Water Purification System, WPS). After fertilizer production, the plant is cleaned with water and the resulting effluent stream, from now on referred to as feed stream of the WPS, rich in NO_3^- and Cl^-, is sent to a mixer (reference point #0) where recycled water is added. At this stage, also ammonia is added to precipitate the phosphate present as calcium phosphates, which are removed upon settling. After the settler (reference point #1), the stream is divided in two equal streams, with one stream recycled to the fertilizer plant, and the other sent to a scrubber (reference point #2), where gaseous NO_2 and HNO_3 are washed out before being added to the mixer for the next cycle. When the chloride concentration reaches a certain level, all surplus water is discharged (reference point #3).

The amount of (H)NO_3 removed by the scrubber is negligible compared to the total amount of NO_3^- present at reference point #0. For that reason, the model does not account for the effect of the scrubber on the NO_3^- concentration. Because of this, the outline of Fig. 8 can be simplified into that of Fig. 9. Note that the process now also includes a membrane unit for NO_3^- recovery.

At reference point #0, the feed stream, rich in NO_3^- and Cl^-, is mixed with fresh and recycled water. The volumetric flow of 5 m^3/h leaving the mixer remains constant during all subsequent cycles. After the settler (reference point #1), the stream is sent to a membrane unit responsible for the NO_3^- recovery and producing a permeate stream (reference point #2) that is recycled to the fertilizer plant. Depending on the membrane selectivity, this stream is more or less contaminated with Cl^-. The Cl^- rich retentate stream that results from the membrane unit (reference point #3) is split (reference point #4), with one part, after being scrubbed, recycled to the mixer, and the other part discharged.

In the system, five reference points are distinguished:

- point #0: where fresh water, the feed stream, and the recycled water are mixed;
- point #1: stream leaving the settler before it enters the membrane unit;
- point #2: permeate stream after filtration by the membrane unit;
- point #3: retentate stream after filtration by the membrane unit;
- point #4: retentate stream to be recycled after splitting.

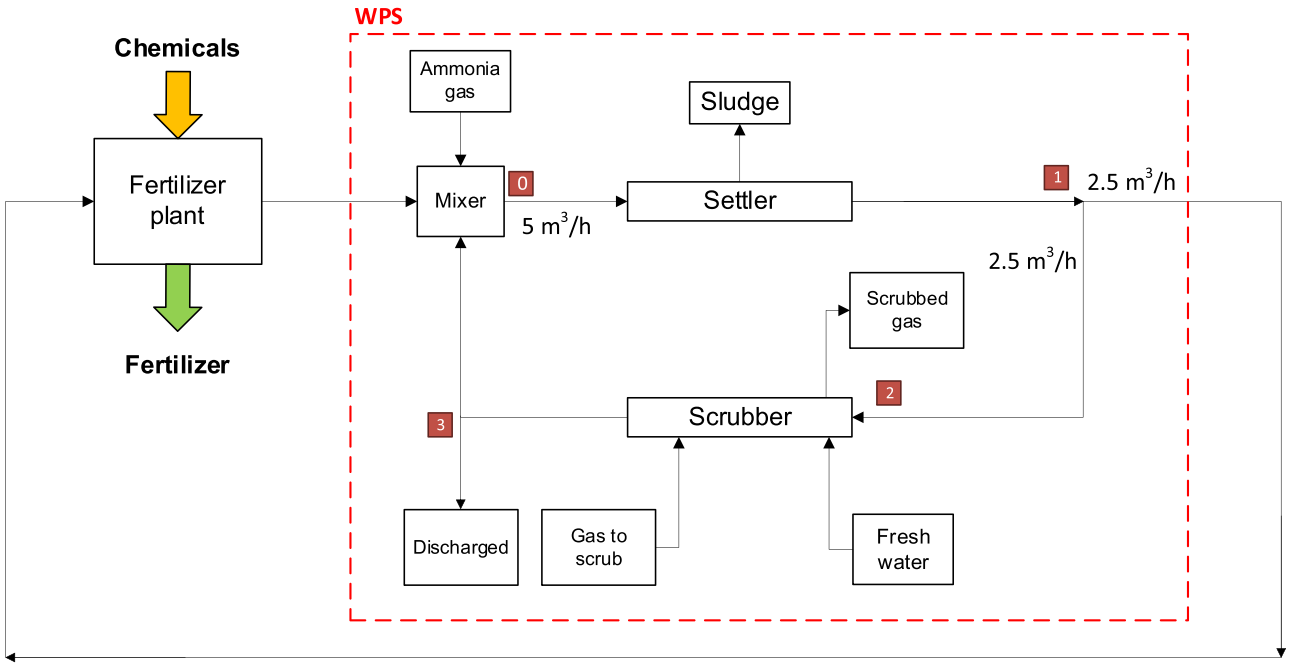

Fig. 8 – Outline of today's Water Purification System (WPS, red dashed box) used in the Porsgrunn NPK fertilizer plant. Reference points #0–3 are further explained in the text.

Similar to the mass balance model presented in Section 2.2, the aim is to calculate the NO_3^-/Cl^- concentration ratio at the five indicated reference points and during each cycle. The fertilizer plant in Fig. 8, Fig. 9 and Fig. 10 is simplified to a unit into which chemicals enter and from which fertilizer is produced. More detailed information regarding this part of the process is beyond the scope of this study. However, one critical parameter is the Cl^- concentration in the permeate stream (reference point #2), recycled to the fertilizer plant; this should not exceed certain levels, depending on the type of fertilizer produced. Given these allowed limit values, the required (minimum) membrane selectivity can be determined. Regulation of the Cl^- level while recovering NO_3^- and reducing the fresh water consumption was the motivation to perform this study.

3.4.1. *Process parameters*

Fig. 10 shows the basic outline of Fig. 9, now complemented with all relevant process parameters referred to in this study. The parameters are listed in Table 2, including their numerical values. Whereas the NO_3^- concentration in the feed entering the mixer is fairly constant, 2.1 mol/L, the Cl^- concentration varies, depending on the grade of fertilizer produced. As was the case with the generic model discussed in Section 2.2, at the start of each cycle, the volumetric flow at reference point #0 remains constant. For the first cycle, it has been assumed that

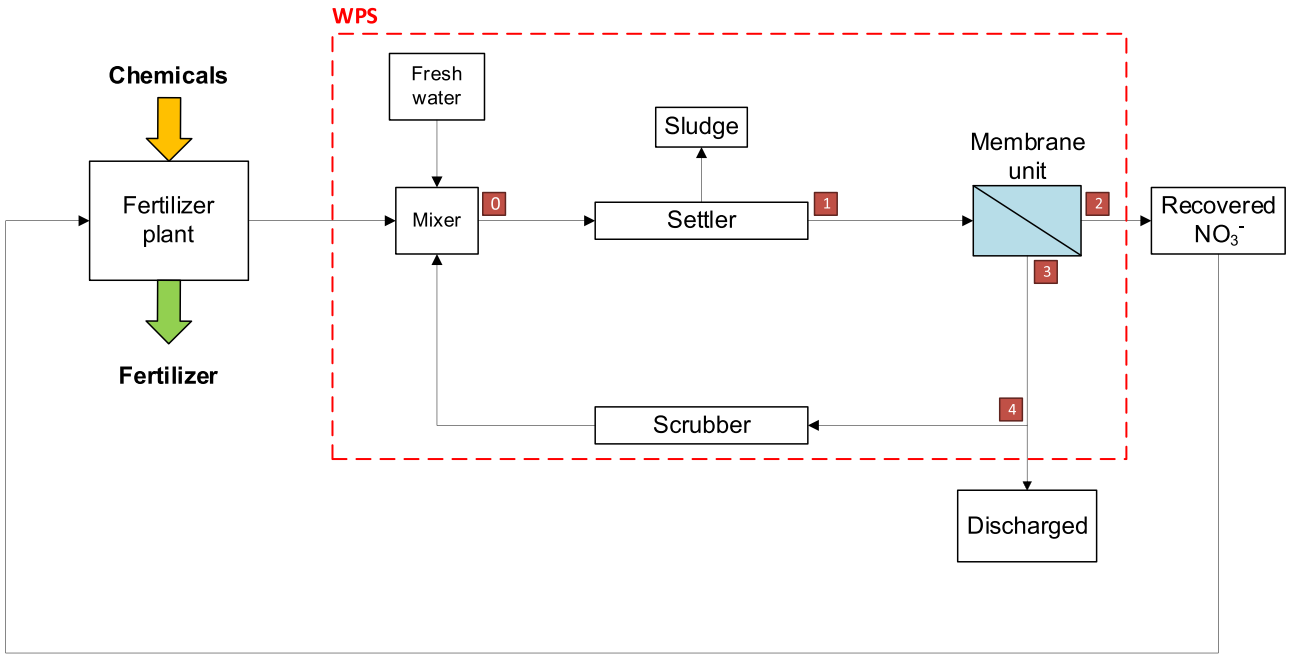

Fig. 9 – Outline of the Water Purification System (WPS, red dashed box) proposed in this study, including a membrane unit for the selective removal of NO_3^-. Reference points #0–4 are further explained in the text.

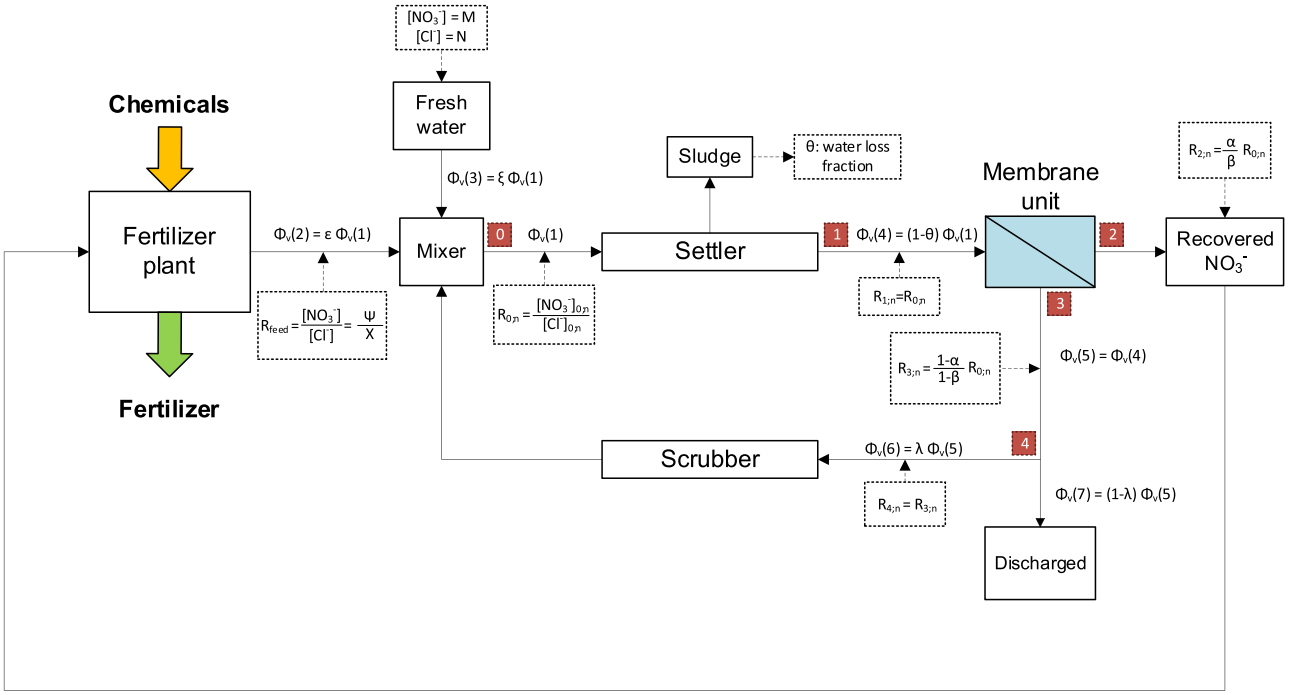

Fig. 10 – Outline of Fig. 9, complemented with the volumetric flows Φv(1)-Φv(7) and the process parameters. Reference points #0–4 are indicated, as well as the relevant (steady-state) volumetric flows.

the composition at point #0 is 50% feed stream and 50% fresh water. In order to minimize the consumption of fresh water, after the first cycle, some of the retentate stream ($\Phi_v(5)$, reference point #3) is recycled to the mixer. As shown in Section 3.3, the fraction of water recycled, λ, influences the Cl^- build-up in the system and, with that, the required membrane selectivity (Fig. 7). Decreasing this fraction decreases the required membrane selectivity to achieve the same NO_3^-/Cl^- ratio in the permeate stream at reference point #2. The flip side of the coin is, however, that reducing λ requires adding more fresh water at point #0, in order to maintain the volumetric flow constant. Therefore, a compromise is needed between the water consumption and the required membrane selectivity. For that reason, the value of λ was arbitrarily set at 0.3. Regarding the fraction of NO_3^- recovered at the membrane unit, the value of α was arbitrarily set at 0.9.

3.4.2. *Mass balance*

The mass balances follow the ones described in Section 2.2. The only difference is that due to a slight water loss at the settler (0.35% of the water stream, $\theta = 0.0035$), Equation 20 is modified into (for n > 1):

$$\xi_n = 1 - \varepsilon_1 - \lambda(1 - \theta) \tag{27}$$

The volumetric flow at reference point #1 becomes:

$$\Phi_v(4) = (1 - \theta)\Phi_v(1) \tag{28}$$

3.4.3. *Required membrane selectivity*

The main purpose of this study is to determine the minimum membrane selectivity (γ_{min}) required to maintain the Cl^- concentration in the permeate stream, recycled to the fertilizer plant, below a certain threshold. As defined by Yara, this limit value is either 4.2 or 9.9 mM, depending on the quality of the fertilizer produced.

As already remarked, whereas the NO_3^- concentration in the feed is fairly constant, the Cl^- concentration varies, ranging from 51 to 200 mM. For that reason, four different combinations of Cl^- in the feed (X) and Cl^- in the permeate at reference point #2 were investigated (case A to D, Table 3). Combining the mass balance of Section 2.2 with the modification proposed in Section 3.4.2 for the Yara process, and the parameters listed in Table 2, it is possible to determine the steady-state Cl^- concentrations at reference point #2 (permeate stream). Fig. 11 shows these Cl^- concentration values for membrane selectivity values ranging from 1 to 40. Given the Cl^- concentration limits, indicated by dashed lines in Fig. 11, this plot allows the determination of the required minimum membrane selectivity (γ_{min}), which values are reported in Table 3.

Lastly, in order to evaluate the influence of water recycling, the selectivity value of 3 reported in Table 3 has been used to calculate the Cl^- concentration in the permeate stream by varying the fraction of water recycled in the WPS, λ. As shown in Fig. 12, a larger water saving is at the expense of Cl^- building up in the system, reflected in a higher Cl^- content in the permeate.

4. Discussion

The current study is primarily focused on the NO_3^-/Cl^- concentration ratio in the permeate (generic model) and the absolute permeate Cl^- concentration of a case study (Yara process). As shown, the values of these two parameters are determined by the interplay of the NO_3^- and Cl^- content in the feed, the permeation properties of the membrane and the fraction of recycled water, to mention the most dominant ones. As our research group (Qian et al., 2020, 2022; Sahin et al., 2022; Singh et al., 2022; Paltrinieri et al., 2019) and others (Kikhavani et al., 2014; Krishna B et al., 2022; Yang et al., 2019; Montes-Rojas et al., 2017; Křivčík et al., 2015; Oh et al., 2014) work on the development of membranes to discriminate between ion species of the same valence, the prime motivation of this investigation was to explore the actual required membrane selectivity for a real-life process.

Table 2 – List of the parameters used for the application under study.

Variables	Description	Value
$\Phi_v(1)$	Volumetric flow at reference point #0	5 m^3/h
Ψ	NO_3^- concentration in the feed	2.1 mol/L
X	Cl^- concentration in the feed	max 0.2 mol/L min 0.051 mol/L
R_{feed}	NO_3^-/Cl^- concentration ratio in the feed: $R = \Psi / X$	41.2 max 10.5 min
$R_{m,n}$	NO_3^-/Cl^- concentration at reference point #m and cycle n	Output
M	NO_3^- concentration in fresh water	0.26 mg/L $4.2 \cdot 10^{-6}$ mol/L
N	Cl^- concentration in fresh water	0.76 mg/L $2.1 \cdot 10^{-5}$ mol/L
ε_1	Fraction of feed stream added at point #0 for the 1st cycle	0.5
ε_n	Fraction of feed stream added at point #0 for cycle number n (n > 1)	0.5
ξ_1	Fraction of fresh water for the 1st cycle	0.5
ξ_n	Fraction of fresh water for cycles number n (n > 1) number n (n > 1)	Equation 25
θ	Fraction of $\Phi_v(1)$ lost due to settling	0.0035
α	Fraction of NO_3^- removed by the membrane system	0.9
β	Fraction of Cl^- removed by the membrane system	$\beta = \frac{\alpha}{\gamma}$
γ	NO_3^- over Cl^- permeation selectivity of the membrane system	$\gamma = \frac{\alpha}{\beta}$
λ	Fraction of water recycled	0.3

Table 3 – Minimum membrane selectivity, γ_{min}, at feed Cl^- concentrations of 51 and 200 mM, required to retain the permeate Cl^- below 4.2 or 9.9 mM. In all cases, the fraction of recycled water (λ) and NO_3^- recovered (α) was set to 0.3 and 0.9, respectively.

Case	$[Cl^-]_{feed}$ (mM)	$[Cl^-]_{permeate}$ limit (mM)	γ_{min}
A	51	9.9	3
B	51	4.2	8
C	200	9.9	13
D	200	4.2	30

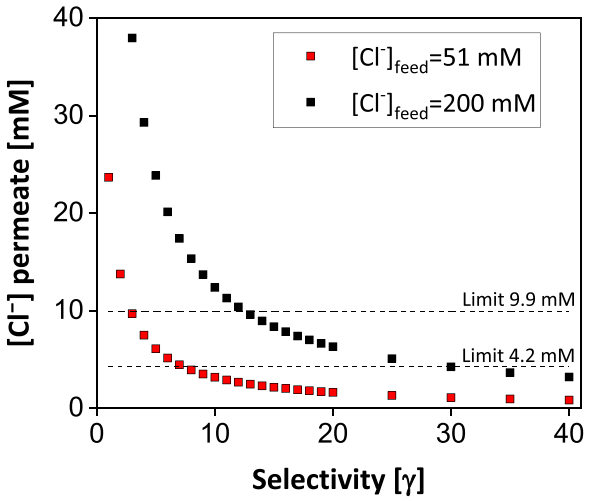

Fig. 11 – Steady-state Cl^- concentration in the permeate stream, $[Cl^-]_{2;n}$, as a function of membrane selectivity, for $\lambda = 0.3$ and $[Cl^-]_{feed} = 51$ mM and 200 mM. Dashed lines indicate the concentration limits of 9.9 mM and 4.2 mM.

Given the calculated selectivity values in Table 3, ranging from 3 to 30, and the highest selectivity value reported by Mubita et al. (2020). of 3, there still is a large margin for improvement. The membranes developed by Mubita et al. (2020). are heterogeneous anion-exchange membranes with low electrical resistance obtained by combining a

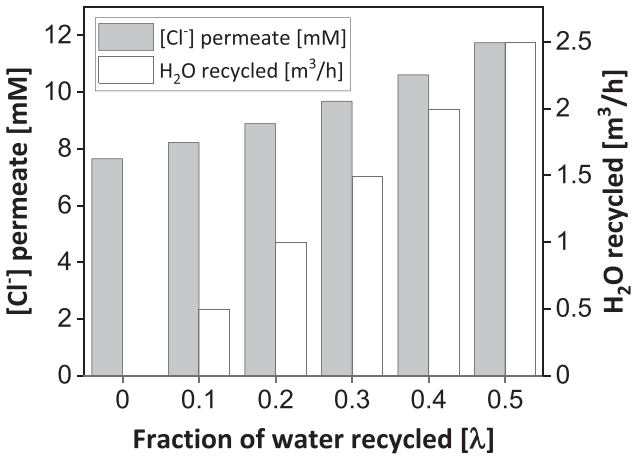

Fig. 12 – Permeate Cl^- content and absolute amount of recycled water in relation to the recycled water fraction, given a total volumetric flow of 5 m^3/h and a (fixed) membrane selectivity of 3.

functionalized polymeric binder and three ion-exchange resins, each containing a different functional group consisting of either trimethyl, triethyl, or tripropyl ammonium moieties. Within this series, the resin with the most hydrophobic functional group, i.e. the tripropyl ammonium, showed the highest NO_3^- over Cl^- permeation selectivity, a value of 3. However, due to the high water content, around 40–50%, it seems rather unlikely that the difference in dehydration energy between NO_3^- and Cl^- is the prominent determinant of the selectivity mechanism of these membranes. For this reason, to match the high selectivity values required for cases B, C and D in Table 3, the development of membranes that fully exploit the difference in dehydration energy between NO_3^- and Cl^-, may be an attractive alternative. Evidently, this approach requires a hydrophobic membrane. Qian et al. (2020, 2022). developed Supported Liquid Membranes (SLM) based on a lipophilic, organic phase impregnated with a borate salt. These SLMs showed a K^+ over Na^+ selectivity, which was attributed to the lower dehydration energy of K^+ (Smith, 1977). Whether this approach can be

extrapolated to anion selectivity has to be seen. Moreover, apart from the relatively high selectivity, issues still to be addressed are the high electrical resistance of SLMs, mainly due to the limited solubility of the borate salt in the organic phase (NPOE), and leakage of the organic compound into the aqueous phase.

Another interesting alternative approach is the one of membranes onto which polyelectrolyte multilayers (PEMs) are assembled using layer-by-layer technology. For example, Yang et al. (Yang et al., 2018) have developed a PEMs membrane with a K^+ over Li^+ selectivity of 7 for use in electrodialysis, and Tekinalp et al. (Tekinalp et al., 2023) have demonstrated that this approach can selectively separate Cl^- and F^- from SO_4^{2-}.

In the context of the difference between cation and anion selectivity, it is worth noting that natural anion channels and transporters exhibit relatively low NO_3^- over Cl^- selectivity (Zifarelli and Pusch, 2010; De Angeli et al., 2006), whereas their cation counterparts can exhibit much higher selectivity values, such as the K^+ over Na^+ selectivity of K^+ channels, which can be as high as 80 (Mita et al., 2021). In general, achieving similar selectivity levels as observed in Nature may require design and synthesis at the atomic, angstrom scale as, for instance, in the case of metal-organic frameworks (Epsztein et al., 2020; Li et al., 2023).

Finally, a word on the incentive of NO_3^- and water recovery. One may argue that apart from sustainability, it is hard to come up with a solid business case for NO_3^- recovery. Indeed, NO_3^- is not a particular expensive chemical (e.g. urea ammonium nitrate price: 687.5 €/Mt on the 28/11/2022 ("Urea Ammonium Nitrate - 2022 Data - 2012–2021 Historical - 2023 Forecast - Price."), but there is certainly more to say about the economics involved. First, fertilizer production is associated with enormous energy consumption. More than 1% of the worldwide produced energy is used to fuel the Haber-Bosch process (Capdevila-Cortada, 2019), i.e., the reduction of N_2 to NH_3, a key compound for fertilizer production. Secondly, in order to promote a healthy environment, (European) legislation moves in the direction of zero discharge ("River basin management - Water - Environment - European Commission.", 2022). Therefore, it is believed that salt discharge will turn out costly in the near future, and investment in water purification systems mandatory. Even more, because nutrient recovery implies water savings as well.

5. Conclusion

Here we show the general outline of a membrane-based process aiming to combine NO_3^- recovery from a waste stream also containing Cl^- with water saving. The key process parameters were identified as the NO_3^-/Cl^- ratio in the feed (R), the fraction of feed NO_3^- that is recovered (α), the fraction of recycled water (λ), and the NO_3^- over Cl^- permeation selectivity of the membrane (γ). For instance, increasing the fraction of recovered NO_3^- (α) or the fraction of recycled water (λ) both decrease the purity of the recovered NO_3^-. Process optimization, therefore, asks for prioritizing aims. When applied to a real-life process, four combinations of process parameters were evaluated, resulting in membrane selectivity values ranging from 3 to 30, while assuming that 90% of the NO_3^- is recovered and 30% of the water recycled. Experimentally, the most serious challenge is developing membranes with high selectivity. One of the strategies discussed to achieve such high values is based on exploiting the difference in dehydration energy between NO_3^- and Cl^-, and for this reason, we hypothesized that the membrane used in the process is hydrophobic.

Declaration of Competing Interest

The authors declare that they have no known competing financial interests or personal relationships that could have appeared to influence the work reported in this paper.

Acknowledgements

The authors thank the Dutch Research Council – Wetsus Partnership Programme on Sustainable Water Technology for funding this project (ALWET.2019.004).This work was performed in the cooperation framework of Wetsus, European Centre of Excellence for Sustainable Water Technology (www.wetsus.nl). Wetsus is co-funded by the Dutch Ministry of Economic Affairs and Ministry of Infrastructure and Environment, the European Union Regional Development Fund, the Province of Fryslan and the Northern Netherlands Provinces. The authors like to thank the participants of the research theme "Desalination" for the fruitful discussions and their financial support. We are especially grateful to Yara (The Netherlands) for all their advice and support. We also would like to thank Dr Porada (Wrocław University of Science and Technology, Poland and Wetsus, The Netherlands) for fruitful discussions and two anonymous reviewers for commenting on earlier versions of this paper.

Appendix A. Supporting information

Supplementary data associated with this article can be found in the online version at doi:10.1016/j.cherd.2023.03.038.

References

"Agri-environmental indicator - mineral fertiliser consumption." ⟨https://ec.europa.eu/eurostat/statistics-explained/index.php?title=Agri-environmental_indicator_-_mineral_fertiliser_consumption⟩ (accessed Nov. 28, 2022).

Capdevila-Cortada, M., 2019. Electrifying the Haber–Bosch. 1055–1055, Dec. Nat. Catal., vol. 2 (12). https://doi.org/10.1038/s41929-019-0414-4

De Angeli, A., et al., 2006. The nitrate/proton antiporter AtCLCa mediates nitrate accumulation in plant vacuoles (Aug.). Nature, vol. 442 (7105), 939–942. https://doi.org/10.1038/nature05013

Dodds, W.K., Smith, V.H., 2016. Nitrogen, phosphorus, and eutrophication in streams. Inland Waters, vol. 6 (2), 155–164. https://doi.org/10.5268/IW-6.2.909

Epsztein, R., DuChanois, R.M., Ritt, C.L., Noy, A., Elimelech, M., 2020. Towards single-species selectivity of membranes with subnanometre pores. Nat. Nanotechnol. 6, 426–436. https://doi.org/10.1038/s41565-020-0713-6

Essien, E.E., et al., 2022. Drinking-water nitrate and cancer risk: a systematic review and meta-analysis. Arch. Environ. Occup. Health, vol. 77 (1), 51–67. https://doi.org/10.1080/19338244.2020.1842313

Kikhavani, T., Ashrafizadeh, S.N., Van Der Bruggen, B., 2014. Nitrate selectivity and transport properties of a novel anion exchange membrane in electrodialysis. Electrochim. Acta, vol. 144, 341–351. https://doi.org/10.1016/j.electacta.2014.08.012

Krishna B, A., Zwijnenberg, H.J., Lindhoud, S., de Vos, W.M., 2022. Sustainable K+/Na+ monovalent-selective membranes with

hot-pressed PSS-PVA saloplastics (Jun.). J. Membr. Sci., vol. 652, 120463. https://doi.org/10.1016/j.memsci.2022.120463
Křivčík, J., Neděla, D., Hadrava, J., Brožová, L., 2015. Increasing selectivity of a heterogeneous ion-exchange membrane. Desalin. Water Treat., vol. 56 (12), 3160–3166. https://doi.org/10.1080/19443994.2014.980970
Kyriakou, V., Garagounis, I., Vourros, A., Vasileiou, E., Stoukides, M., 2020. An electrochemical haber-bosch process (Jan.). Joule, vol. 4 (1), 142–158. https://doi.org/10.1016/j.joule.2019.10.006
Li, X., et al., 2023. Construction of angstrom-scale ion channels with versatile pore configurations and sizes by metal-organic frameworks (Jan.). Nat. Commun., vol. 14 (1), 286. https://doi.org/10.1038/s41467-023-35970-x
Mita, K., Sumikama, T., Iwamoto, M., Matsuki, Y., Shigemi, K., Oiki, S., 2021. Conductance selectivity of Na^+ across the K^+ channel via Na^+ trapped in a tortuous trajectory (Mar.). Proc. Natl. Acad. Sci., vol. 118 (12), e2017168118. https://doi.org/10.1073/pnas.2017168118
Montes-Rojas, A., Rentería, J.A.Q., Chávez, N.B.J., Ávila-Rodríguez, J.G., Soto, B.Y., 2017. Influence of anion hydration status on selective properties of a commercial anion exchange membrane electrochemically impregnated with polyaniline deposits. RSC Adv., vol. 7 (41), 25208–25219. https://doi.org/10.1039/C7RA03331A
Mubita, T., Porada, S., Aerts, P., van der Wal, A., 2020. Heterogeneous anion exchange membranes with nitrate selectivity and low electrical resistance. J. Membr. Sci., vol. 607, 118000. https://doi.org/10.1016/j.memsci.2020.118000
B.J. Ni et al., *CHAPTER 16: Denitrification Processes for Wastewater Treatment*, vol. 2017-Janua, no. 9. The Royal Society of Chemistry, 2017. doi: ⟨10.1039/9781782623762–00368⟩.
Nightingale, E.R., 1959. Phenomenological theory of ion solvation. effective radii of hydrated ions (Sep). J. Phys. Chem., vol. 63 (9), 1381–1387. https://doi.org/10.1021/j150579a011
Oh, C.-M., Hwang, C.-W., Hwang, T.-S., 2014. Synthesis of a quaternarized poly(vinylimidazole-co-trifluoroethylmethacrylate-co-divinylbenzene) anion-exchange membrane for nitrate removal (Dec.). J. Environ. Chem. Eng., vol. 2 (4), 2162–2169. https://doi.org/10.1016/j.jece.2014.09.014
Omara, P., Aula, L., Oyebiyi, F., Raun, W.R., 2019. World cereal nitrogen use efficiency trends: review and current knowledge. Agrosystems Geosci. Environ., vol. 2 (1), 1–8. https://doi.org/10.2134/age2018.10.0045
Paltrinieri, L., et al., 2019. Functionalized anion-exchange membranes facilitate electrodialysis of citrate and phosphate from model dairy wastewater. Environ. Sci. Technol., vol. 53 (5), 2396–2404. https://doi.org/10.1021/acs.est.8b05558
Qian, Z., Miedema, H., Sahin, S., de Smet, L.C.P.M., Sudhölter, E.J.R., 2020. Separation of alkali metal cations by a supported liquid membrane (SLM) operating under electro dialysis (ED) conditions (Dec.). Desalination, vol. 495. https://doi.org/10.1016/j.desal.2020.114631
Qian, Z., Miedema, H., de Smet, L.C.P.M., Sudhölter, E.J.R., 2022. Permeation selectivity in the electro-dialysis of mono- and divalent cations using supported liquid membranes (Jan.). Desalination, vol. 521. https://doi.org/10.1016/j.desal.2021.115398
"River basin management - Water - Environment - European Commission." ⟨https://ec.europa.eu/environment/water/water-framework/index_en.html⟩ (accessed Nov. 28, 2022).
Sahin, S., Zuilhof, H., Zornitta, R.L., de Smet, L.C.P.M., 2022. Enhanced monovalent over divalent cation selectivity with polyelectrolyte multilayers in membrane capacitive deionization via optimization of operational conditions (Jan.). Desalination, vol. 522, 115391. https://doi.org/10.1016/j.desal.2021.115391
Sata, T., 2000. Studies on anion exchange membranes having permselectivity for specific anions in electrodialysis - Effect of hydrophilicity of anion exchange membranes on permselectivity of anions. J. Membr. Sci., vol. 167 (1), 1–31. https://doi.org/10.1016/S0376-7388(99)00277-X
Singh, K., Sahin, S., Gamaethiralalage, J.G., Zornitta, R.L., de Smet, L.C.P.M., 2022. Simultaneous, monovalent ion selectivity with polyelectrolyte multilayers and intercalation electrodes in capacitive deionization (Mar.). Chem. Eng. J., vol. 432, 128329. https://doi.org/10.1016/j.cej.2020.128329
Skendžić, S., Zovko, M., Živković, I.P., Lešić, V., Lemić, D., 2021. The impact of climate change on agricultural insect pests (May). Insects, vol. 12 (5). https://doi.org/10.3390/insects12050440
Smith, D.W., 1977. Ionic hydration enthalpies (Sep.). J. Chem. Educ., vol. 54 (9), 540. https://doi.org/10.1021/ed054p540
Sodaye, S., Suresh, G., Pandey, A.K., Goswami, A., 2007. Determination and theoretical evaluation of selectivity coefficients of monovalent anions in anion-exchange polymer inclusion membrane (May). J. Membr. Sci., vol. 295 (1), 108–113. https://doi.org/10.1016/j.memsci.2007.02.044
Tekinalp, Ö., Zimmermann, P., Burheim, O.S., Deng, L., 2023. Designing monovalent selective anion exchange membranes for the simultaneous separation of chloride and fluoride from sulfate in an equimolar ternary mixture (Jan.). J. Membr. Sci., vol. 666, 121148. https://doi.org/10.1016/j.memsci.2022.121148
"Urea Ammonium Nitrate - 2022 Data - 2012–2021 Historical - 2023 Forecast - Price." ⟨https://tradingeconomics.com/commodity/urea-ammonium⟩ (accessed Nov. 28, 2022).
Vaselbehagh, M., Karkhanechi, H., Takagi, R., Matsuyama, H., 2016. Effect of polydopamine coating and direct electric current application on anti-biofouling properties of anion exchange membranes in electrodialysis (Oct.). J. Membr. Sci., vol. 515, 98–108. https://doi.org/10.1016/j.memsci.2016.05.049
Wang, X., et al., 2020. Emergent constraint on crop yield response to warmer temperature from field experiments (Nov.). Nat. Sustain., vol. 3 (11), 908–916. https://doi.org/10.1038/s41893-020-0569-7
Ward, M.H., et al., 2018. Drinking water nitrate and human health: an updated review. Int. J. Environ. Res. Public. Health, vol. 15 (7), 1–31. https://doi.org/10.3390/ijerph15071557
"World Population Prospects 2019 Highlights.pdf." Accessed: Nov. 28, 2022. [Online]. Available: ⟨https://population.un.org/wpp/publications/files/wpp2019_highlights.pdf⟩.
Yang, L., Tang, C., Ahmad, M., Yaroshchuk, A., Bruening, M.L., 2018. High selectivities among monovalent cations in dialysis through cation-exchange membranes coated with polyelectrolyte multilayers (Dec.). ACS Appl. Mater. Interfaces, vol. 10 (50), 44134–44143. https://doi.org/10.1021/acsami.8b16434
Yang, S., et al., 2019. Codeposition modification of cation exchange membranes with dopamine and crown ether to achieve high K^+ electrodialysis selectivity (May). ACS Appl. Mater. Interfaces, vol. 11 (19), 17730–17741. https://doi.org/10.1021/acsami.8b21031
Ye, Y., et al., 2018. A critical review on ammonium recovery from wastewater for sustainable wastewater management (no. July). Bioresour. Technol., vol. 268, 749–758. https://doi.org/10.1016/j.biortech.2018.07.111
Zifarelli, G., Pusch, M., 2010. CLC transport proteins in plants (May). FEBS Lett., vol. 584 (10), 2122–2127. https://doi.org/10.1016/j.febslet.2009.12.042